EVOLUTION

Exceptional preservation of organs in Devonian placoderms from the Gogo lagerstätte

Kate Trinajstic[1,2]*, John A. Long[3,4], Sophie Sanchez[5,6], Catherine A. Boisvert[1], Daniel Snitting[5], Paul Tafforeau[6], Vincent Dupret[5], Alice M. Clement[3], Peter D. Currie[7], Brett Roelofs[1], Joseph J. Bevitt[8], Michael S. Y. Lee[3,9], Per E. Ahlberg[5]

The origin and early diversification of jawed vertebrates involved major changes to skeletal and soft anatomy. Skeletal transformations can be examined directly by studying fossil stem gnathostomes; however, preservation of soft anatomy is rare. We describe the only known example of a three-dimensionally mineralized heart, thick-walled stomach, and bilobed liver from arthrodire placoderms, stem gnathostomes from the Late Devonian Gogo Formation in Western Australia. The application of synchrotron and neutron microtomography to this material shows evidence of a flat S-shaped heart, which is well separated from the liver and other abdominal organs, and the absence of lungs. Arthrodires thus show the earliest phylogenetic evidence for repositioning of the gnathostome heart associated with the evolution of the complex neck region in jawed vertebrates.

The Gogo lagerstätte shows exceptional three-dimensional bone and muscle preservation within placoderms (*1*–*3*), a paraphyletic taxon of stem gnathostomes (*4*, *5*). Preservation occurred through bacterially mediated authigenic mineralization under conditions of photic zone euxinia [(*6*) and supplementary text]. The discovery that this process also preserved internal organs in arthrodires reveals a virtually unknown aspect of vertebrate evolution. Early gnathostome internal organs are unknown outside of digestive tract infills (*7*–*9*) and blood vessel impressions in the antiarch placoderm *Bothriolepis* (*8*–*10*). Using propagation phase contrast synchrotron x-ray microtomography (PPC-SRμCT) and neutron tomography, arthrodire organs can be visualized in three dimensions and distinguished from bones and mineral matrix (Fig. 1, A to E, and fig. S1). Internal viscera are preserved in approximate life position, although they have undergone postmortem shrinkage (figs. S2 and S3 and supplementary text). All organs have been recovered from multiple specimens (supplementary materials), but no single specimen shows a full complement, which is consistent with decay experiments (*11*).

[1]School of Molecular and Life Sciences, Curtin University, Bentley, WA 6102, Australia. [2]Western Australian Museum, Welshpool, WA 6106, Australia. [3]College of Science and Engineering, Flinders University, Adelaide, SA 5001, Australia. [4]Museum Victoria, Melbourne, VIC 3001, Australia. [5]Department of Organismal Biology, Evolutionary Biology Center, Uppsala University, 75236 Uppsala, Sweden. [6]European Synchrotron Radiation Facility, 38000 Grenoble, France. [7]Australian Regenerative Medicine Institute and EMBL Australia, Monash University, Clayton, VIC 3800, Australia. [8]Australian Nuclear Science and Technology Organisation (ANSTO), Lucas Heights, NSW 2234, Australia. [9]Earth Sciences Section, South Australian Museum, Adelaide, SA 5000, Australia.
*Corresponding author. Email: k.trinajstic@curtin.edu.au

An asymmetrical structure comprising a small dorsal chamber, a larger ventral pyramid-shaped chamber, and an anterior tube-like extension lies at the back of the pharyngeal cavity in a ventral midline position (Fig. 1 and movie S1). It is not a cavity infilling because empty space borders the external surfaces (Fig. 1, A to D). It is interpreted as a heart because of its orthotopic position, S-shaped configuration, two chambers, and an outflow tract. The anterior tubular structure is interpreted as the conus arteriosus, which is anterior to the ventricle with the atrium dorsolateral to the ventricle (Fig. 1, H to J, and fig. S4). Unlike in *Rhacolepis* (*12*), the sinus venosus or conal valves cannot be distinguished. There is no evidence of the cartilaginous or ossified pericardial capsule present in lampreys and osteostracans (*13*). Fanning out from the heart are a nexus of anteroposteriorly oriented, linear structures, rounded in cross section (movie S2), which are interpreted as the median ventral aorta with associated vessels (Fig. 1, F and G, and fig. S4, K and L).

Posterior to the body wall, occupying a ventral position and extending to the midpoint of the posterior ventrolateral plate, are two distally tapering lozenge-shaped structures (Fig. 2, A to C, and fig. S5). A broad anterior margin is preserved, evidently natural, and transverse to the long axis of the body. The bilobed nature of the structure, its size, and its ventral position in the anterior part of the abdomen indicate that this is the liver. The left lobe is approximately three-fourths the size of the right (Fig. 2C). The lobes were likely medially joined in life, as they are separated by a gap of less than 1 mm in WAM 95.1.1 (fig. S6A). The lobes of the liver from the Famennian shark *Ferromirum oukherbouchi* have been similarly separated postmortem (*14*).

A conicospiral tubular structure (Fig. 2, A, G, and H, and figs. S1I and S7, A to C) extends along the axis of the body to the level of the pelvic girdle. The spiral arrangement, extension through the abdominal region, and comparable morphology to the spiral intestine of *Bothriolepis* (*7*) confirms it as the spiral intestine. The posterior portion of the intestine widens, and isolated parts of the arthropod *Montecaris gogoensis* (*15*) have been identified within (fig. S8). The ventral position at the terminal end of the intestine, posterior to the posterior ventrolateral plates, and the presence of digested contents confirm that this is the rectum.

Anterior to the intestine, a rectangular sack-like structure lies slightly right of the midline resting directly on the liver (Fig. 2A). The ventral wall is ruptured, likely due to the gases from decomposition (Fig. 2I), but the thick anterodorsal wall and anterior margin are preserved (Fig. 2, I to L). Tomography reveals the walls of this structure to be smooth externally but rugose internally (Fig. 2, D and E). The rugose internal surface is exposed in the acid-prepared specimen WAM 95.1.1 (Fig. 2F). On the basis of its position dorsal to the liver, its rugose internal surface, and its smooth external surface, the structure is identified as the stomach. An identical structure has been recovered from a similar position within *Rhacolepis* sp. (*16*).

Lungs or a swim bladder are present in most extant osteichthyans but absent in all chondrichthyans (*13*). Chondrichthyans use a large oily liver as a buoyancy organ (supplementary text). This suggests that lungs are an osteichthyan autapomorphy, but the alleged presence of lungs in the antiarch placoderm *Bothriolepis* (*7*–*9*) has been used to argue that lungs are a jawed vertebrate innovation subsequently lost in chondrichthyans. Extant sarcopterygians (including tetrapods) and the lung-breathing actinopterygians (*17*) demonstrate that lungs, if present, should lie ventrolateral to the stomach. However, no remnants of lung-like structures can be observed in this region, although this might reflect poor preservation potential of lung tissue. The phylogenetic position of antiarchs in the gnathostome stem group is usually considered stemward to arthrodires (*4*) (Fig. 3 and figs. S9 and S10) but has also been proposed to be crownward (*5*). If lungs are indeed absent in arthrodires but present in antiarchs, this would be more consistent with the heterodox crownward position of antiarchs. However, the morphology of the supposed "lungs" in *Bothriolepis* (*9*) is incompatible with the functionally necessary presence of a narrow anterior trachea in the lungs of osteichthyans. The recognition of a postbranchial lamina in antiarchs [Yunnanolepididae (*18*)] and here in *Bothriolepis* (fig. S11 and supplementary text) supports

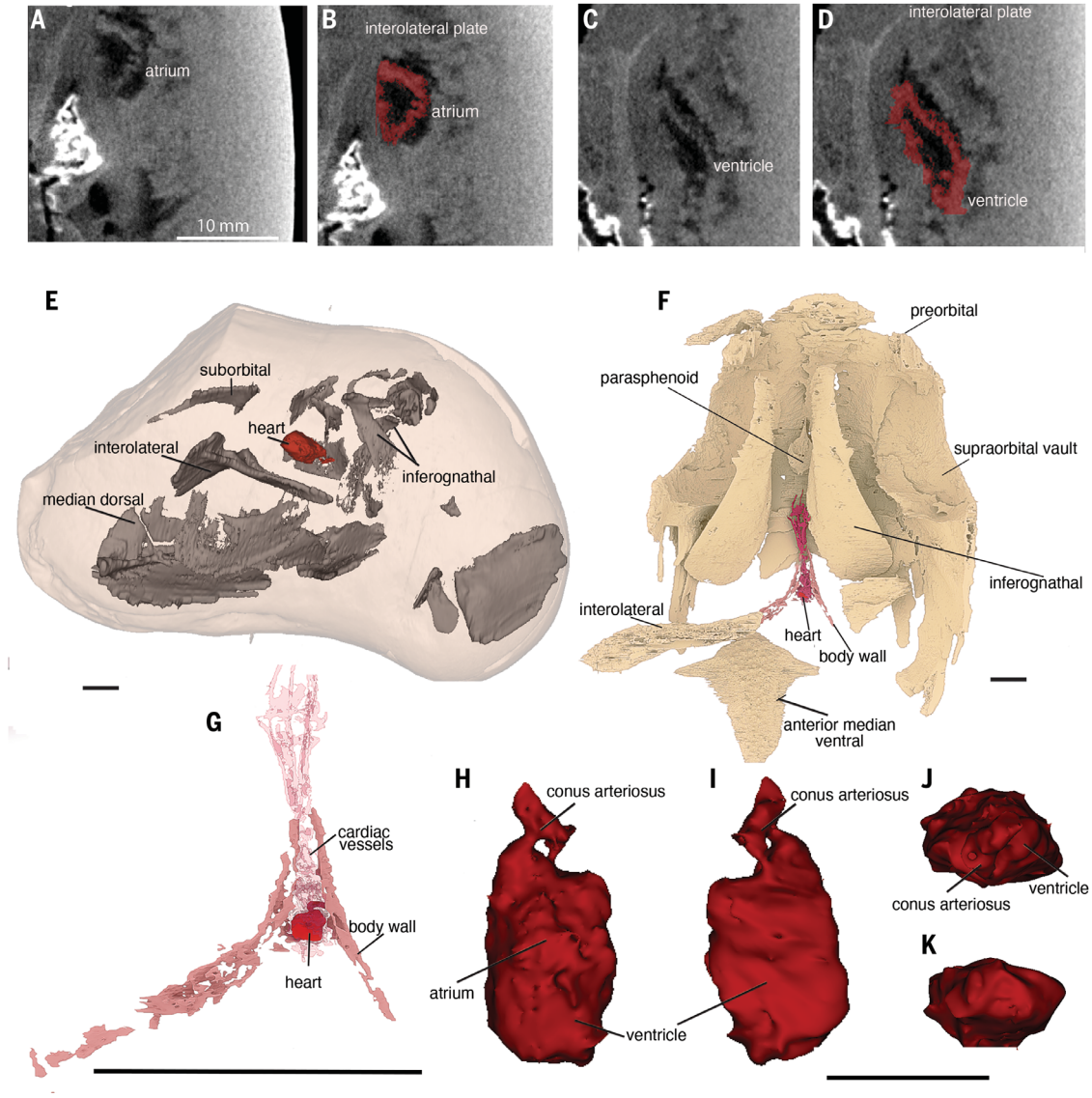

Fig. 1. The morphology of the cardiac region in arthrodires. (**A** to **D**) The heart modeled from NTμCT WAM 2020.2.1, showing the atrium (A), atrium colored red (B), ventricle (C), and ventricle colored red (D). (**E**) Carbonate nodule showing the relationship of the heart to the dermal plates. (**F** and **G**) Pericardial region modeled from PPC-SRμCT MV P230859 with the dermal plates modeled (F) and showing the heart and cardiac vessels only (G). (**H** to **K**) The heart showing detail of the conus arteriosus, atrium, and ventricle modeled from NTμCT of WAM 2020.2.1 in dorsal (H), ventral (I), anterior (J), and posterior (K) view. Scale bars, 1 cm.

the notion that the paired bilobed organ in *Bothriolepis* occupied the identical position to the liver in arthrodires (Fig. 3). Therefore, we conclude that this structure is the liver, and that both antiarchs and arthrodires lack evidence of lungs. This implies a single origin of lungs, above both these stem taxa, and potentially as late as in the Osteichthyes (Fig. 3).

Our fossil data also provide evidence for a dorsal shift of the heart atrium and the repositioning of the heart anterior to the caudal wall of the branchial chamber (Fig. 3 and supplementary text). In jawless fishes, the atrium and ventricle are lateral to each other (*19*) and the heart is posterior to the branchial field (Fig. 3). In chondrichthyans and fish-like osteichthyans, the atrium is dorsal to the ventricle, the heart is level (anteroposteriorly) with the branchial chamber, the bones of the shoulder girdle are close to the branchial arches, and the hypobranchial and cucullaris muscles connect these bones to the skull, resulting in narrow neck (*20*). In antiarchs, the heart is posterior to the branchial lamina (Fig. 3) and the nuchal gap separating the dorsal head and trunk armor is absent (fig. S11E), as is the cucullaris muscle (*8*, *20*, *21*). Arthrodires possess an anteriorly positioned heart underneath the branchial arches, nuchal gap, and cucullaris muscles (*1*) (Fig. 4). These traits show that arthrodires share the crown gnathostome morphology to the exclusion of antiarchs and thus support the conventional arrangement of a paraphyletic Placodermi with arthrodires more crownward than antiarchs (Fig. 3). Recent studies in extant gnathostomes have shown that the progenitor cells of the hypobranchial and

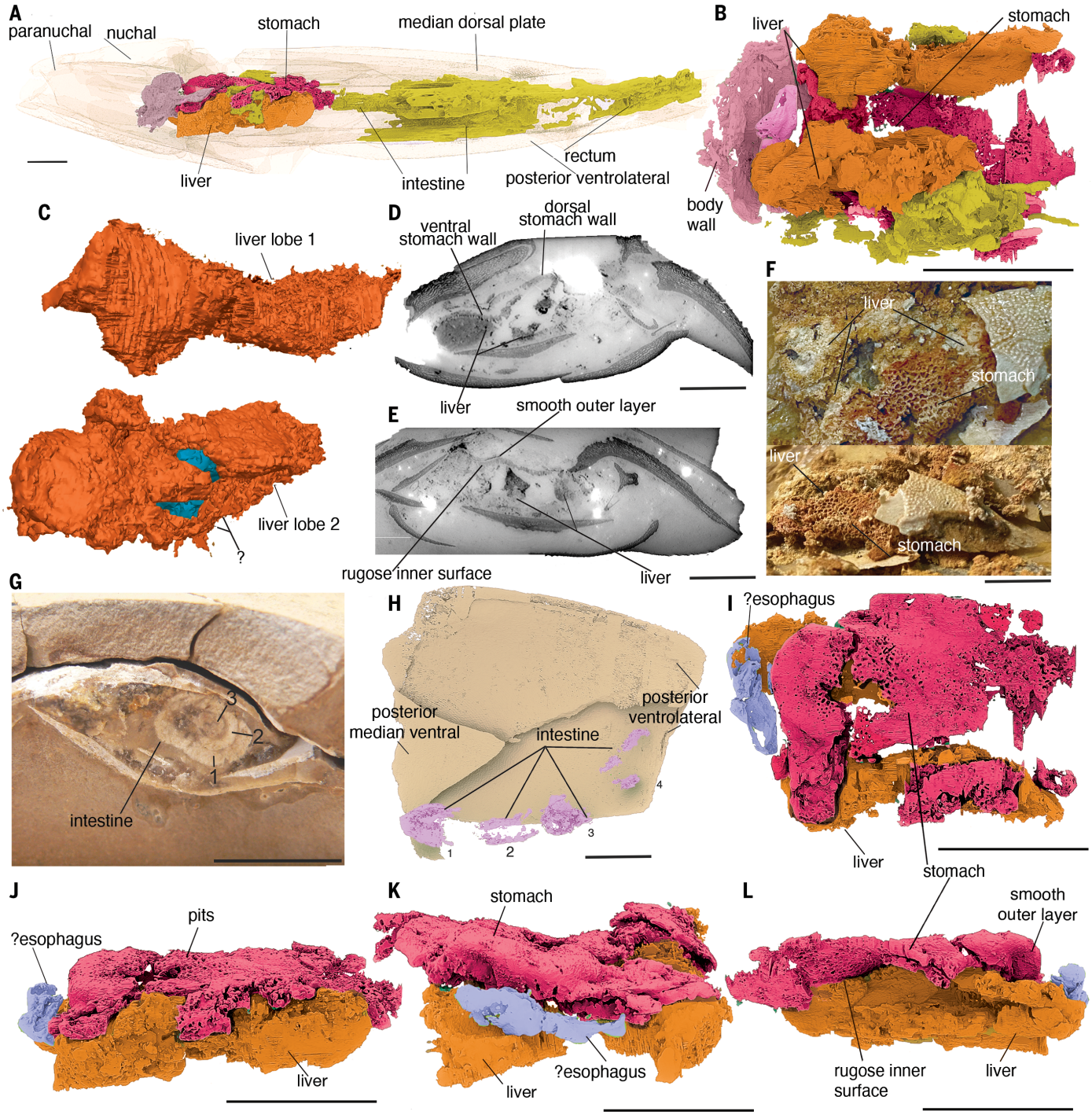

Fig. 2. The abdominal viscera preserved in arthrodires. (**A**) The position of the abdominal organs in relation to the dermal plates modeled from PPC-SRμCT MV P230859 (lateral view). (**B**) Three-dimensional model from MV P230859 showing the liver and stomach. (**C**) Liver in dorsal view. (**D**) Anterior tomographic slice of the liver and stomach (MV P230859). (**E**) Posterior tomographic slice. (**F**) Ventral stomach wall and liver (WAM 95.1.1). (**G**) Spiral valves of the intestine (WAM 09.4.1), transverse view. (**H**) Dorsal view modeled from PPC-SRμCT WAM 09.4.1. Numbers 1 to 4 indicate the layers of the spiral valve from outer (1) to inner (4). (**I** to **L**) Morphology of the liver and stomach modeled from PPC-SRμCT MV P230859 in dorsal (I), lateral (J), anterior (K), and ventrolateral (L) view. Scale bars, 1 cm.

cucullaris muscles are shared by the cardiac muscle (*22*) and that the shifting of the head-trunk interface and elongation of the neck is driven by gain of function of the newly duplicated *Tbx5* gene [(*23*) and supplementary text]. Our fossil data support the hypothesis that the anterior repositioning of the heart and development of the neck are not restricted to crown gnathostomes but were both present in the lineage leading to arthrodires and crown gnathostomes. Notably, they are absent in antiarchs.

Together with the previously described musculature (*1*), the three-dimensionally preserved organs make the Gogo arthrodires the most

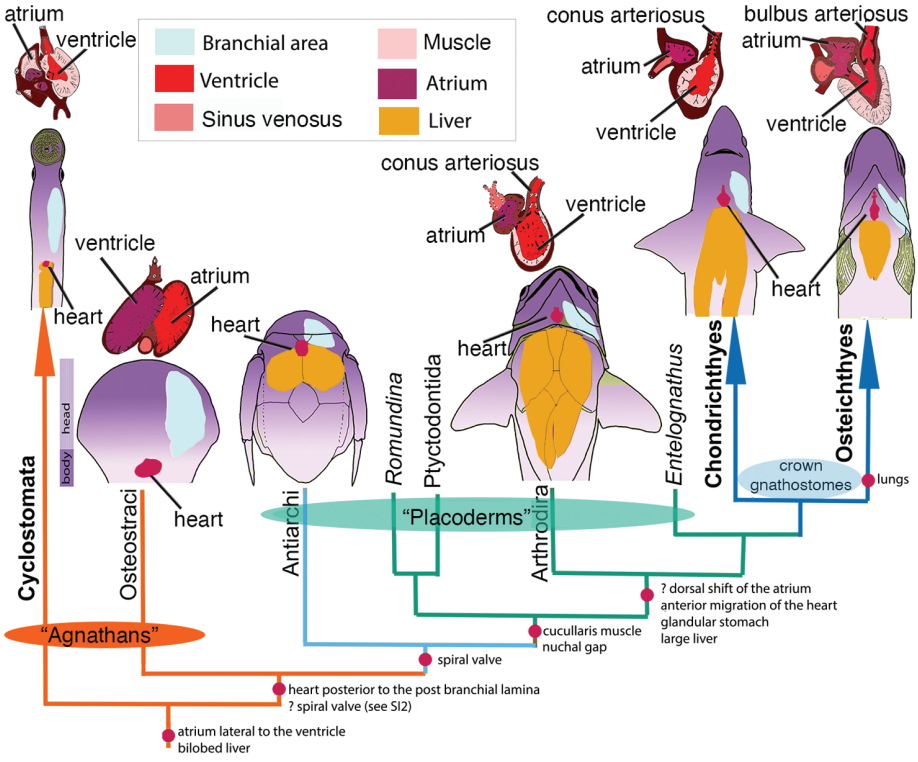

Fig. 3. A phylogenetic framework of the lower vertebrates. The proposed sequence of evolution for organs preserved within arthrodires is indicated [simplified from fig. S14 and adapted from figure 1 of (*1*)].

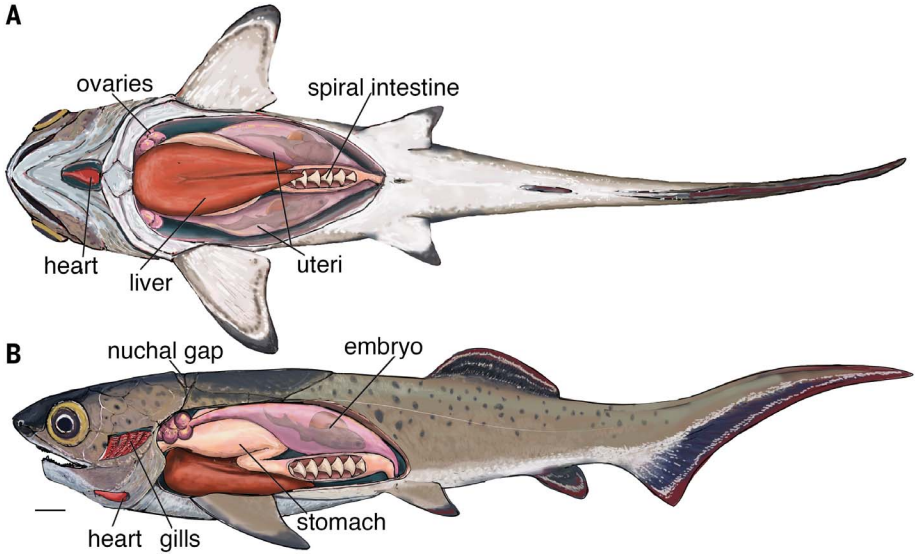

Fig. 4. Reconstruction of arthrodire internal anatomy. (**A**) Lateral view; (**B**) ventral view. The reconstruction is based on preserved organs recovered from WAM 2020.2.1 and MV P230859 and embryos recovered from P50934. Scale bar, 1 cm.

fully understood of all jawed stem gnathostomes, help to resolve conflicting phylogenies for early fish, and can validate evolutionary transition hypotheses generated by extant developmental models (*20*, *22*, *23*). They provide a unique window on jawed vertebrate evolution just before the origin of the crown group and the assembly of the gnathostome body plan.

REFERENCES AND NOTES

1. K. Trinajstic *et al.*, *Science* **341**, 160–164 (2013).
2. K. Trinajstic, C. Marshall, J. Long, K. Bifield, *Biol. Lett.* **3**, 197–200 (2007).
3. J. A. Long, K. Trinajstic, *Annu. Rev. Earth Planet. Sci.* **38**, 255–279 (2010).
4. B. King, T. Qiao, M. S. Y. Lee, M. Zhu, J. A. Long, *Syst. Biol.* **66**, 499–516 (2017).
5. Y. A. Zhu *et al.*, *Curr. Biol.* **31**, 1112–1118.e4 (2021).
6. I. Melendez *et al.*, *Geology* **41**, 123–126 (2013).
7. R. H. Denison, *J. Paleontol.* **15**, 553–561 (1941).
8. M. Arsenault, S. Desbiens, P. Janvier, J. Kerr, in *Recent Advances in the Origin and Early Radiation of Vertebrates*, G. Arratia, M. V. H. Wilson, R. Cloutier, Eds. (Pfeil, Munich, 2004), pp. 439–445.
9. P. Janvier, S. Desbiens, J. A. Willett, *J. Vertebr. Paleontol.* **27**, 709–710 (2007).
10. D. Goujet, *C. R. Palevol* **10**, 323–329 (2011).
11. S. E. Gabbott, R. S. Sansom, M. A. Purnell, *Palaeontology* **64**, 789–803 (2021).
12. L. Maldanis *et al.*, *eLife* **5**, e14698 (2016).
13. P. Janvier, *Early Vertebrates* (Oxford Univ. Press, 1996).
14. L. Frey, M. I. Coates, K. Tietjen, M. Rücklin, C. Klug, *Commun. Biol.* **3**, 681 (2020).
15. D. E. G. Briggs, W. I. Rolfe, P. D. Butler, J. J. Liston, J. K. Ingham, *J. Syst. Palaeontology* **9**, 399–424 (2011).
16. P. R. Wilby, D. M. Martill, *Hist. Biol.* **6**, 25–36 (1992).
17. N. Tatsumi *et al.*, *Sci. Rep.* **6**, 30580 (2016).
18. Y. Wang, M. Zhu, *PeerJ* **6**, e4808 (2018).
19. P. Janvier, L. R. Percy, I. C. Potter, *J. Zool.* **223**, 567–576 (1991).
20. N. Adachi, J. Pascual-Anaya, T. Hirai, S. Higuchi, S. Kuratani, *Zool. Lett.* **4**, 1–3 (2018).
21. R. Ericsson, R. Knight, Z. Johanson, *J. Anat.* **222**, 67–78 (2013).
22. E. Heude *et al.*, *eLife* **7**, e40179 (2018).
23. H. Higashiyama *et al.*, *J. Morphol.* **277**, 1146–1158 (2016).

ACKNOWLEDGMENTS

We acknowledge the Gooniyandi people, the traditional owners on whose land the fossils were collected. We thank the Western Australian Museum and Museum of Victoria for assistance with curation and access to collections. **Funding:** Supported by Australian Research Council grants DP1092870 and ARC-DP140104161 (J.A.L., K.T.), DP1096002 (C.A.B., P.D.C.), ARC-DP110101127 (K.T.), and ARC-DP200103219 (P.D.C., K.T.); European Research Council Advanced Investigator grant 233111 (P.E.A., V.D., S.S.); the Knut and Alice Wallenberg Foundation (P.E.A.); European Synchrotron proposal EC-203 (P.E.A., S.S., K.T.); and Australian Neutron proposal P5203 (A.M.C., J.A.L., K.T.). **Author contributions:** Conceptualization: K.T., J.A.L., P.E.A. Methodology: All authors. Investigation: K.T., J.A.L., S.S., V.D., P.D.C., P.E.A. Visualization: S.S., C.A.B., P.T., D.S., V.D., A.M.C., J.J.B. Funding acquisition: K.T., J.A.L., S.S., A.M.C., P.D.C., P.E.A. Project administration: K.T., C.A.B. Writing: All authors. **Competing interests:** The authors declare no competing interests. **Data and materials availability:** All fossils are accessioned in public collections and, upon curator approval, are available for study by qualified researchers. All (other) data needed to evaluate the conclusions of the paper are presented in the paper or the supplementary materials. Raw CT scans of fossils scanned at ESRF are deposited in the ESRF database (http://paleo.esrf.eu/). Neutron scan data is available in the paleontological microtomographic database MorphoSource at www.morphosource.org/concern/media/000381874?locale=en.

SUPPLEMENTARY MATERIALS

science.org/doi/10.1126/science.abf3289
Provenance Statement
Materials and Methods
Supplementary Text
Figs. S1 to S14
References (*24*–*64*)
Movies S1 and S2
Data S1 to S4

Submitted 20 January 2021; resubmitted 9 January 2022
Accepted 16 August 2022
10.1126/science.abf3289